Taylor & Francis
Taylor & Francis Group

REVIEW

Nucleolar ribosomal RNA synthesis continues in differentiating lens fiber cells until abrupt nuclear degradation required for ocular lens transparency

Danielle Rayêe [a], U. Thomas Meier [b], Carolina Eliscovich [c], and Aleš Cvekl [a]

aDepartments of Ophthalmology and Visual Sciences and Genetics, Albert Einstein College of Medicine, Bronx, NY, USA; bDepartment of Cell Biology, Albert Einstein College of Medicine, Bronx, NY, USA; cDepartments of Medicine (Hepatology) and Developmental and Molecular Biology, Albert Einstein College of Medicine, Bronx, NY, USA

ABSTRACT

Cellular differentiation requires highly coordinated action of all three transcriptional systems to produce rRNAs, mRNAs and various 'short' and 'long' non-coding RNAs by RNA Polymerase I, II and III systems, respectively. RNA Polymerase I catalyzes transcription of about 400 copies of mammalian rDNA genes, generating 18S, 5.8S and 28S rRNA molecules. Lens fiber cell differentiation is a unique process to study transcriptional mechanisms of individual crystallin genes as their very high transcriptional outputs are directly comparable only to globin genes in erythrocytes. Importantly, both terminally differentiated lens fiber cells and mammalian erythrocytes degrade their nuclei through different mechanisms. In lens, the generation of the organelle-free zone (OFZ) includes the degradation of mitochondria, endoplasmic reticulum, Golgi apparatus and nuclei. Here, using RNA fluorescence *in situ* hybridization (FISH), we evaluated nascent rRNA transcription, located in the nucleoli, during the process of mouse lens fiber cell differentiation. Lens fiber cell nuclei undergo morphological changes including chromatin condensation prior to their denucleation. Remarkably, nascent rRNA transcription persists in all nuclei that are in direct proximity of the OFZ. Additionally, changes in both nuclei and nucleoli shape were evaluated via immunofluorescence detection of fibrillarin, nucleolin, UBF and other proteins. These studies demonstrate for the first time that highly condensed lens fiber cell nuclei have the capacity to support nascent rRNA transcription. Thus, we propose that 'late' production of rRNA molecules and consequently of ribosomes increases crystallin protein synthesis machinery within the mature lens fibers.

Introduction

Eukaryotic cells have three distinct transcriptional systems known as RNA polymerase I, II and III [1]. The RNA Polymerase I transcribes about 400 copies of rDNA genes in mammalian genomes to generate individual mature 18S, 5.8S and 28S rRNA molecules from a single primary transcript [2] within the nucleoli component of the nucleus [3]. Nucleoli are membrane-less nuclear sub-compartments [4,5] composed of the granular component (GC), the dense fibrillar component (DFC) and the fibrillar centre (FC) [6–9]. Transcription of rRNA occurs between the FC and DFC compartments [10,11]. Following rRNA processing, the resulting mature rRNA molecules are incorporated as both the catalytical and structural components of the large and small ribosomal subunits within the nucleolus, forming complete ribosomes [12]. The mouse rDNA genomic sequences [13], located on short arms of acrocentric chromosomes (12, 15, 16, 17, 18 and 19), represent the most evolutionarily conserved domains of the genome [7,14]. In contrast, the RNA Polymerase II generates mRNAs from over 23,000 protein coding genes in addition to a growing list of long and short non-coding RNAs

(ncRNAs) [15]. Finally, the RNA Polymerase III generates 5S rRNA, tRNAs and various snRNAs, and plays a role in homologous repair of DNA double-stranded breaks [16,17]. In an average mammalian cell, rRNAs comprise 80–90% of transcripts, while mRNAs are only ~4% of the total transcripts, and other RNAs (tRNAs, lncRNAs, snRNA, snoRNAs, eRNAs and miRNAs) make up the rest of the total RNA pool [2,18]. The three-dimensional (3D) chromatin landscape/architecture within individual nuclei and its subsequent role in transcription of individual genes is cell type-specific. This represents one of the most intricate biological puzzles: to understand the coordinated action of these complex machineries that regulate transcription, DNA replication and DNA repair [19,20].

Cell growth and proliferation are proportional to the rate of protein synthesis driven by ribosome biogenesis [21,22]. Individual cells invest major resources into the ribosome synthesis to promote growth and differentiation. This resource allocation then changes when the cell terminally differentiates. However, there is a unique situation during terminal differentiation shared by mammalian erythrocytes

and ocular lens fiber cells in which they abruptly degrade their nuclei [23,24]. In lens, the nuclei, located in the central sub-region of the lens fiber cell compartment, gradually change their shape and size followed by their abrupt physical disintegration [25–27]. In contrast, the mammalian erythrocyte nuclei are extruded from the cells into the macrophages as an 'enucleation' process [24,28]. This unique lens fiber cell denucleation process is essential for lens transparency along with a robust accumulation of individual α- and β/-crystallin proteins. Crystallin proteins are encoded by 16 mouse genes and accumulate in the cytoplasm of lens fiber cells where they reach a concentration of 450 mg/ml [29]. Thus, the lens is an excellent system to examine the molecular mechanism required for both tissue-specific and maximal transcriptional and translational outputs [29].

We have shown earlier that expression of crystallin genes is comparable to that of globin genes in red blood cells, while other highly expressed genes, such as insulins (Ins1 and Ins2) and α2-HS glycoprotein (Ahsg) and transferrin (Trf) are expressed in much lower levels in the pancreas and liver, respectively [30]. Unexpectedly, our analysis of nascent mRNA expression of βA1- and γA-crystallin mRNAs revealed that their expression peaks within the lens fiber cell nuclei just prior to their destruction. In contrast, the transcription of the αA-crystallin genes, generating the most abundant lens proteins, peaked much earlier [23]. Strikingly, nearly 60% of nuclei just prior to their degradation showed expression of at least one γA-crystallin (Cryga) allele with biallelic expression found in more than 25% of nuclei. Visualization of transcriptionally active RNA Polymerase II enzymes found a few large condensates in these nuclei concomitant with active transcription of multiple crystallin genes [23]. However, nothing is known about nascent transcription catalysed by RNA Polymerase I within the lens fiber cell nucleoli.

To produce ribosomes, the RNA Polymerase I system [31] requires a major portion of the cell's energy and resources [14,21,32]. However, the operations of lens fiber cell transcriptional-translational machinery are limited by the denucleation process and limited blood supply [29]. Degradation of mitochondria, endoplasmic reticulum and Golgi apparatus was visualized earlier in terminally differentiating mouse lens fiber cells [33]. Importantly, depletion of BCL2 interacting protein 3-like (Bnip3l/Nix) in lens, a regulator of mitophagy, causes retention of mitochondria, endoplasmic reticulum and Golgi apparatus [33]. The degradation of the transient vascular systems located both at the anterior and posterior portions of the lens represents another challenge for lens terminal differentiation [34–36]. Thus, it is possible that rRNA production may be attenuated earlier, reduced, or kept at high levels until the nuclear degradation takes place depending on how the lens fiber cells evolved to manage their precious resources required for the generation of ribosomes and subsequently crystallin proteins [29].

Earlier studies of the lens fiber cell nuclei revealed changes in nuclear shape from ovoid nuclei in lens epithelial cells and in early elongating lens fibers into more rounded nuclei located near the OFZ [25,37]. As is seen in mammalian erythrocytes [24], these nuclei show chromatin condensation, transfer of histone and non-histone proteins into the cytoplasm and reduction in size; however, lens nuclei undergo an abrupt fragmentation within the cytoplasm as shown in detail elsewhere [23,38–40]. Previous studies of lens fiber cell nucleoli and rRNA transcription are limited to general studies of nuclear and nucleolar morphology [37,41,42], identification of ribosome clusters in the vicinity of nucleoli in nuclei near the OFZ [42], changes in fibrillarin (located in the DFZ) in differentiating lens fiber cells [37], analysis of half-life of rRNAs via visualization of ribosomes [43] and detection of the 47S pre-rRNAs in proliferating cells of the adult mouse lens epithelium [44].

To generate new insights into the biology of the nucleolus during lens fiber cell differentiation, here we analysed various proteins located both in the nucleolus and nucleus in combination with RNA FISH to visualize both nascent rRNA transcription and mature rRNAs during mouse lens embryogenesis. The results clearly show that nuclei next to the OFZ are capable of nascent rDNA transcription catalysed by RNA Polymerase I and, thus, retain functional nucleoli.

Results

Visualization of nuclear morphology, fibrillarin and nucleolin through the progressive stages of mouse lens fiber cell differentiation

The 3D-structure of the mouse lens, including the OFZ, is shown in Figure 1A. To follow the lens fiber cell differentiation, the lens fiber cell compartment of the newborn lens can be divided into four symmetric sub-regions a, b, c and d (Figures 1B,C) to aid the initial spatial visualization of gradual changes in the nuclear morphology within the concentric zones of lens fiber cells at various stages of their terminal differentiation [23]. Lens fiber cells then undergo dramatic elongation from areas a to d, and F-actin filaments are reorganized as these cells enter the OFZ (Figure 1D) as summarized elsewhere [46,47]. Regions a, b, c and d represent postmitotic early differentiated fiber cells, intermediate fiber cells, advanced fiber cells and predenucleated cells, respectively. At late embryonic stage E18.5, the OFZ is not yet fully established, and area d comprises lens fiber cells at late differentiation phase (Figure 1B). In the newborn lens (P0.5), the OFZ is in the centre of the tissue (Figure 1C) and nuclear morphology changes are visible throughout each stage of fiber cells differentiation (Figure 1C - compare enlarged DAPI stained nuclei). In area a, there are abundant oval-shaped nuclei, whereas areas b and c display more rounded nuclei that are undergoing chromatin condensation. In the outer subregions of area d, small scattered nuclear remnants are found.

To explore how primary and secondary fiber cells change their nuclear and nucleolar morphologies throughout their differentiation process, we first analysed cells in areas a, b, c and d using immunofluorescence to visualize fibrillarin (rRNA 2'-O-methyltransferase, 34.3 kDa) as the canonical marker of the nucleolus/DFC, and lamin B1 of the inner nuclear membrane, at embryonic stages E14.5 and E16.5. At E14.5, the majority of the lens fiber cell compartment is formed from the 'primary' lens fiber cells originating from the posterior cells of the lens vesicle (E11-E11.5) via cell cycle exit-coupled terminal differentiation [48]. At E14.5, both the
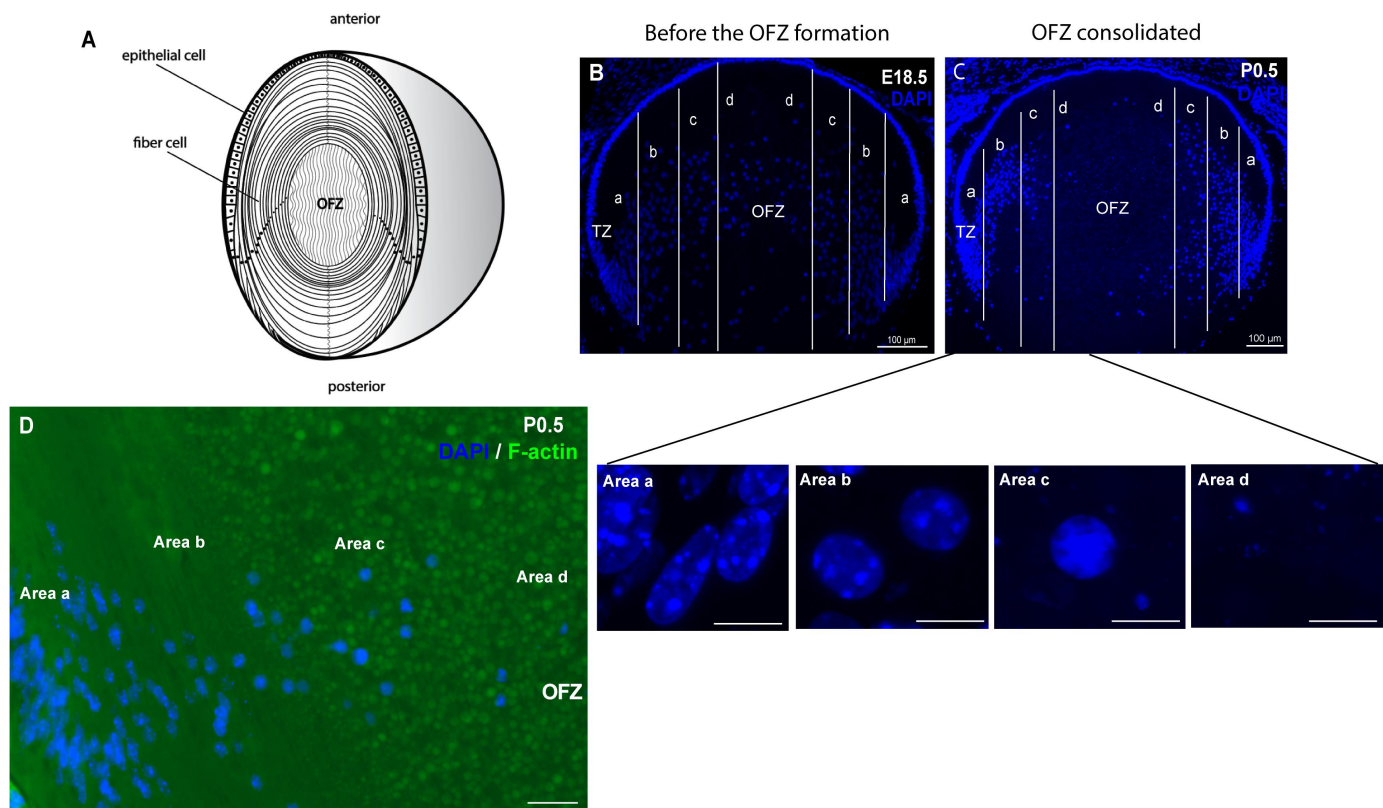
Figure 1. Mouse lens morphology and nuclear changes throughout differentiation. (A) 3D- and cross-section sketch of the mammalian lens [29,45]. Organelle free zone, OFZ. (B) The E18.5 lens is symmetrically divided into areas a, b, c and d from the transition zone (TZ, cells exiting cell cycle and undergoing the earliest stages of terminal differentiation) to the imminent organelle free zone (OFZ), that is still developing. (C) The P0.5 newborn lens displaying the fully formed OFZ within the area d, with no remaining nuclei in that area. Inserts from areas a-d show nuclear morphological changes prior to denucleation. Area a is marked by abundant elongated nuclei, area b shows intermediate fiber cells prior to the nuclear condensation. Area c shows nuclear condensation and complete nuclear disintegration is shown in the area d. (D) F-actin (green) cytoskeleton organization of fibre cells from areas a to d, which represents the formation of the OFZ. dapi-stained nuclei (blue, panels B-D). Inserts scale bars = 10 μm.

areas a and b are marked by two or three nucleoli per nucleus as observed by the fibrillarin stainings (Figure 2A). The nuclear morphology is overall elongated throughout all areas a-d at this stage (Figure 2B). No differences in intranuclear fibrillarin intensity were found between E14.5 and E16.5 in areas a and b (Supplementary Figure S2), however elongated nuclei are still detected in areas a-b within emerging 'secondary' lens fiber cells (E16.5). In contrast, nuclei in areas c-d formed by primary lens fibers exhibit a more rounded shape and marks of nuclear condensation (Figures 2C,D). These trends are further highlighted at E18.5 where the embryonic lenses display stretched-shaped nuclei found in areas a and b, forming the secondary lens fiber cells, with abundant nucleoli staining (Figures 3A,B). At E18.5, fiber cells in area d clearly show signs of nuclear condensation and nucleoli co-localize with DAPI-reduced nuclear regions (Figures 3A,B). Finally, the newborn (P0.5) lenses have a fully formed OFZ in area d (Figure 3D). Fibrillarin staining shows that the cells in areas a and b display multiple large nucleoli within a single nucleus. In comparison, some nuclei in area c are highly condensed within a rounded shape; nevertheless, normal nucleoli stainings are present (Figures 3C,D). During advanced lens fiber cell differentiation, the nuclear shape drastically shifts from an elongated to a round-shaped from area a to areas b and c (Figure 3D).

Nucleolin (77 kDa) is a major nucleolar protein, comprised of four RNA-binding domains and a C-terminal RGG-rich 'tail'. It is also located in the nucleoplasm, where it is known to play a role in ribosome assembly/maturation [49]. Importantly, nucleolin co-localizes with the nucleoli during active transcription [50]. We observed that nucleolin signal co-localizes with the nucleolus throughout areas a-d in the mouse E14.5, E16.5 and E18.5 embryonic fibre cells (Figures 4A,C). Nuclei displaying more than one nucleolus are frequently seen in all these four areas. Nevertheless, nucleolar numbers per each nucleus remain consistent throughout the embryonic and final stages of lens fiber cell differentiation (Suplementary Figures S1A,B).

Previous studies of mouse and chick lenses demonstrated active DNA repair in maturing nuclei within the prospective OFZ and adjacent areas [51,52]. To investigate this further, we immunolabelled newborn (P0.5) lens tissue for the histone variant H2AX that is phosphorylated at serine residue 139 (γH2AX) [53]. Nuclei displayed a progressive increase in γH2AX staining in areas b and c (Figure 5A). We next quantified the percentage of γH2AX cells throughout areas a-c. Areas b and c showed a significant increase in the γH2AX positive nuclei across three biological replicates (Figure 5B). These data suggest that fibre cells approaching the OFZ start to display signs
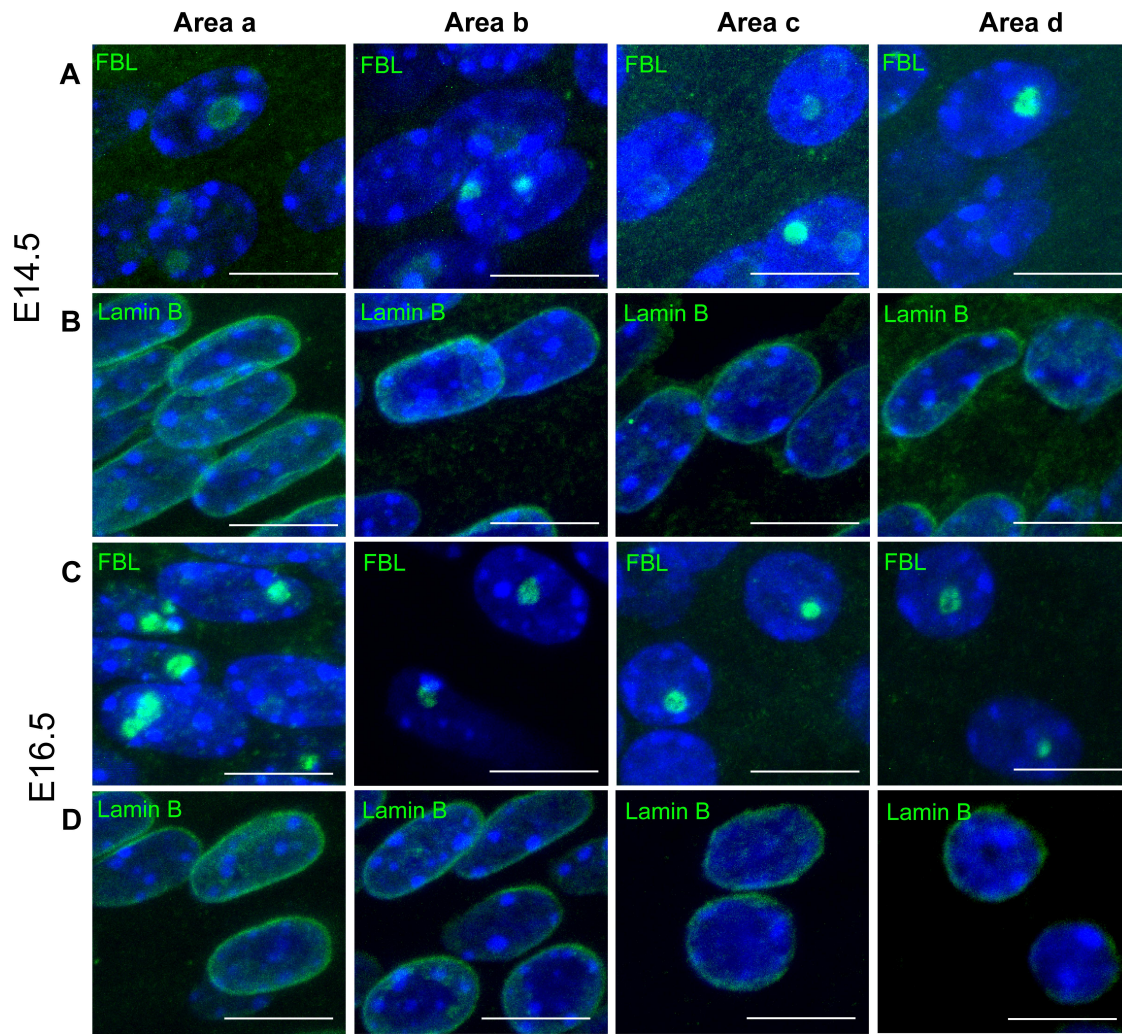
Figure 2. Early stages of differentiation of mouse lens fibre cells (E14.5 and E16.5). Immunolabeling of fibrillarin and lamin B (both in green) was performed to show primary (E14.5) and both primary and secondary (E16.5) lens fiber cells nuclei and nucleoli morphology within the lens tissue regions (panels A-D). The segmented areas (a, b, c, d) analysed are shown in Figure 1A. (A–D) Fiber cells in area a display consistently elongated nuclei throughout embryonic stages E14.5 to E16.5. (B) E14.5 lens comprises mostly of primary lens fiber cells that display abundant nucleolar staining. This pattern is also seen in secondary fiber cells in E16.5 and E14.5 where nuclear morphology is mostly elongated whereas, at E16.5 rounded nuclei are seen more frequently in areas c and d. (C, D) E16.5 advanced primary lens fiber cells nuclei display nuclear condensation observed though DAPI and lamin B stainings. DAPI-stained nuclei (blue), scale bars = 10 μm.

of DNA damage and active repair mechanisms in the area b. However, all cells in area c exhibit an increase in nuclear damage/repair prior to denucleation. Taken together, there are gradual changes in the nuclear morphology; specifically, the number of nucleoli and evidence of DNA damage during lens fiber cell terminal differentiation that could have a negative impact on transcription of rRNA.

Nascent and mature rRNAs are generated in nucleoli adjacent to the OFZ

To establish rRNA FISH in the mouse lens, we employed two sets of probes targeting the rRNA internal-transcribed spacers 1 and 2 (ITS1/ITS2 probes) and the 18S and 28S regions (18S/28S probes) of the pre-rRNAs, as described elsewhere [54] (Figure 6A). The ITS1/ITS2 probes localize the nascent nucleolar rRNAs, whereas the 18S/28S probes visualize mature pre-rRNAs that accumulate in the nucleus and are already exported to the cytoplasm within the individual ribosomes.

We first analysed patterns of rRNA signals in embryonic lenses throughout development from E14.5 and E18.5 by *in situ* hybridization with ITS1/ITS2 probes (Figures 6A-C). We observed that fiber cells in area a frequently show more than one nucleolus per nucleus at E16.5 (Figure 6C). Nucleolar rRNA follows similar patterns seen in nucleolar staining with NCL and fibrillarin (Figures 3 and 4). At E18.5, area d, condensed nuclei show nascent rRNA transcription (Figure 6D).

Pre-rRNAs (ITS1/ITS2 probes) co-localizing with nucleoli in areas a and b within newborn lenses were observed (Figure 7A, top; Figure 7B, top). Importantly, the nuclei located in areas c and d also display nascent rRNAs in their nucleoli as well (Figure 7A,B top and bottom). We were able to detect the ITS1/ITS2 signals even in highly condensed nuclei located in area c. In area d representing OFZ, no intranuclear signal was detected as expected. Mature rRNAs detected via the 18S/28S probes are abundant in the nuclei in areas a and b of the newborn mouse lens (Figure 8A, bottom).
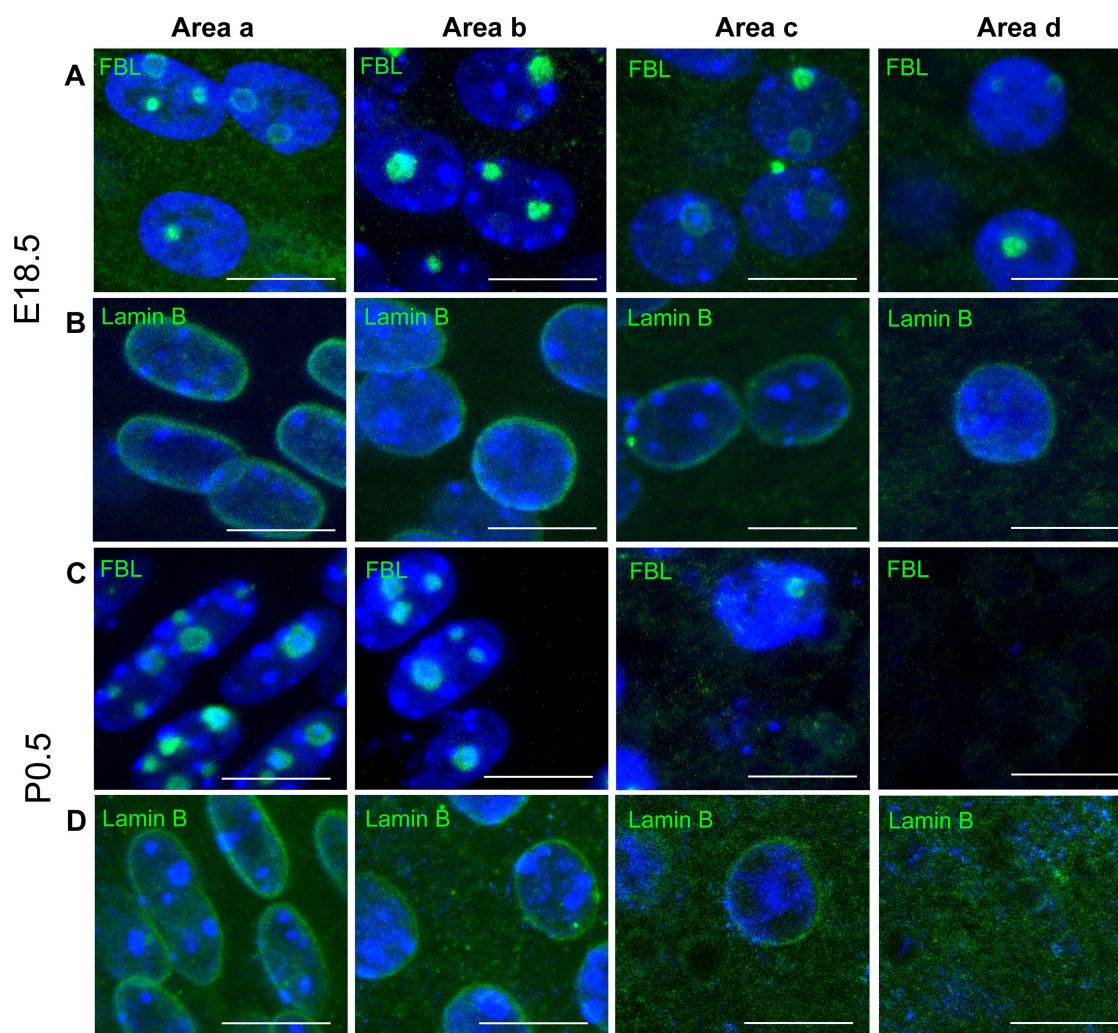
Figure 3. The final stages of lens fiber cells differentiation (E18.5 and P0.5) are marked by nuclear disassembly. (A–D) E18.5 and P0.5 lenses displaying elongated nuclei in area a, and several nucleoli co-localizing with fibrillarin. (A, B) in the area b, there is a mixed population of cells transitioning into the center of the lens tissue. (A–D) in the area c fiber cells start displaying first signs of nuclear condensation at E18.5; however, these morphological changes are more apparent in newborn lens (bottom). (C) Nucleolar structure (green) remains intact in fiber cells at advanced stage of differentiation (white arrowheads in area c). The nuclear envelope (green) is observed in late degenerated nuclei in area c. (A, D) sparse nuclei are found in the area d of E18.5 lens tissue whereas at P0.5 the OFZ is already formed. dapi-stained nuclei (blue), scale bars = 10 μm.

Nuclei displaying more than one nucleolus were also often observed within areas a and b. High cytoplasmic rRNA FISH signals were also detected using the 18S/28S probe set (Figures 7A,B bottom). These data demonstrate that the mature rRNAs are present in the cytoplasm of lens fiber cells after the programmed nuclear destruction.

Next, we quantified the nucleolar signals observed throughout areas a-c for both nascent and mature rRNAs via the ITS and 18S/28S probes, respectively. We found that areas a, b and c display comparable numbers of nascent rRNAs co-localizing with the nucleoli (Figure 8A). Interestingly, the quantities of mature rRNAs in the nucleus of cells in areas a, b and c have also not shown significant differences (Figure 8B). Our data also show that cells in area c display comparable numbers of both nascent and mature rRNAs to the cells in area a, representing the earliest stages of lens fiber cells differentiation. In addition, we quantified the mean intensity of the nuclear signals for ITS1/ITS2 and 18S/28S probes throughout areas a and c (Figures 8C,D) and no significant differences were found. Taken together, these quantitative measurements demonstrate that the levels of premature and mature rRNA are maintained invariable from area a to area c in differentiating lens fiber cells.

Transcriptional machineries are maintained prior to the final nuclear disintegration in lens fiber cells

The nuclear condensation and transfer of nuclear proteins to the cytoplasm [23,24] obviously represents a major challenge for normal nuclear function, including transcriptional processes. To gain additional insights, we visualized UBF (Upstream Binding Transcription Factor), transcriptionally active RNA Polymerase II as a marker of active sites of mRNA expression, and SC-35/Srsf2 protein of the nuclear speckles (Figures 9A-C). UBF is a nucleolar DNA-binding phosphoprotein essential for the proper functioning of RNA Polymerase I transcriptional machinery [55]. We observed the co-localization of UBF with the nuclei of cells in areas a and b (Figure 9B). RNA polymerase II displays a marked co-localization in nuclei of areas a and
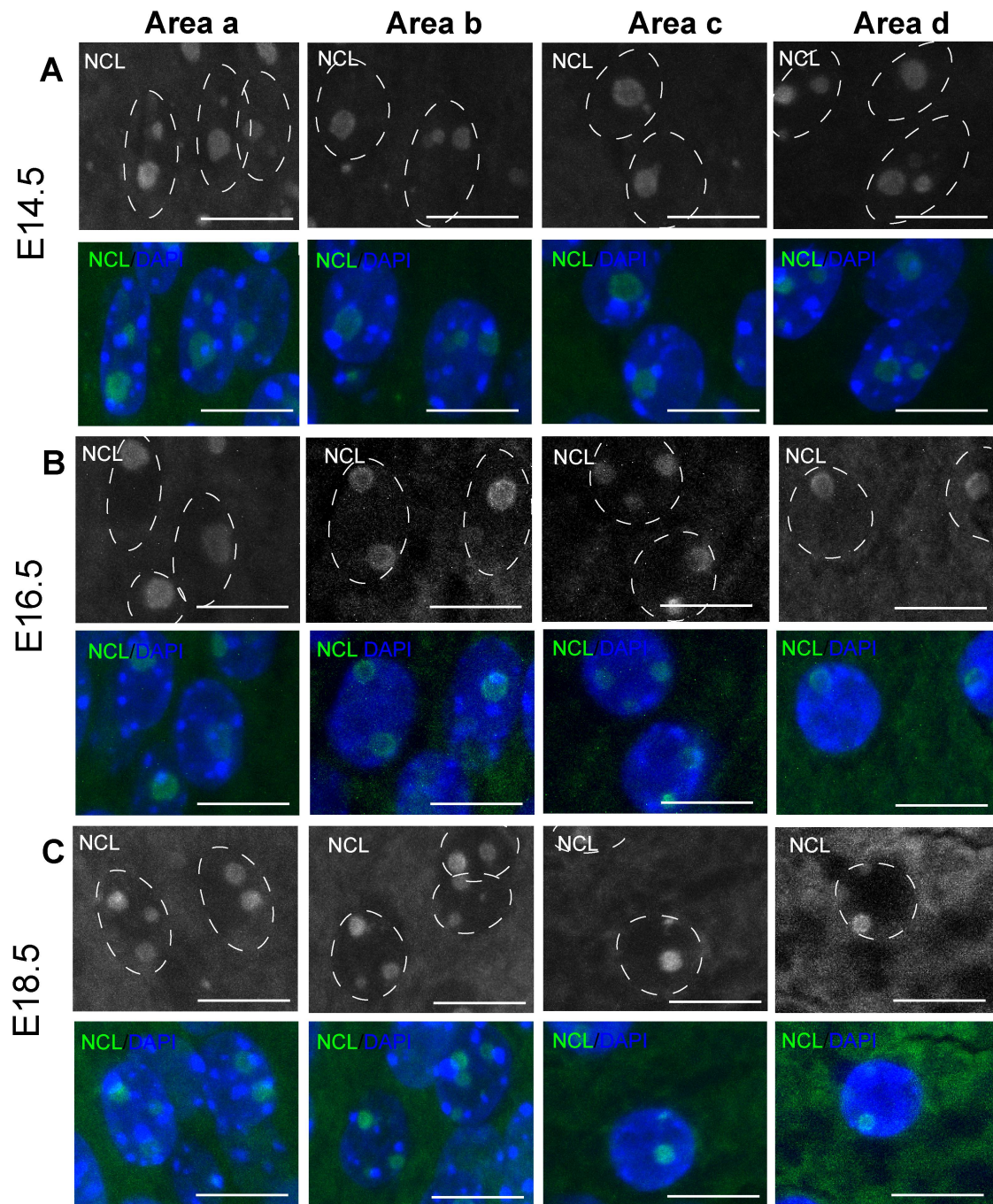
Figure 4. Nucleoli staining in embryonic lens fiber cells. The data show E14.5 (A), E16.5 (B) and E18.5 (C) embryonic stages in areas a, b, c and d. Nucleolin (NCL) and nuclei dotted (top); NCL (green) merged with DAPI-stained nuclei (bottom). Scale bars = 10 μm.

b (Figure 9A). In area c, a few strong signals of RNA Polymerase II are detected (Figure 9A). Importantly, our previous studies have shown that these large condensates represent active sites of crystallin gene transcription [23]. Nuclear speckles represent hubs that spatially link pre-mRNA transcription, splicing and nuclear export [56]. We found that nuclear speckles also co-localized with nucleoli in areas a and b (Figure 9C). Remarkably, nuclei of area c display nucleoli positive staining for all three factors: UBF, RNA Polymerase II and SC-35, within nucleoli (Figures 9A-C). Together, these data, coupled with the

positive nucleolar signals of the rRNA probes (Figure 6), demonstrate that lens fiber cells are actively producing rRNAs in the nucleoli of highly condensed nuclei, just prior to their denucleation.

Finally, to confirm the nucleolar integrity prior to denucleation, we immunolabelled nucleolin (Anti-NCL) and nucleophosmin (Anti-NPM1), two essential nucleolar proteins that are required for ribosome biogenesis [49]. Intranuclear fibrillarin signal intensity in area c also confirms the nucleolar integrity prior denucleation (Suplementary Figure S2). Both nucleolar proteins are
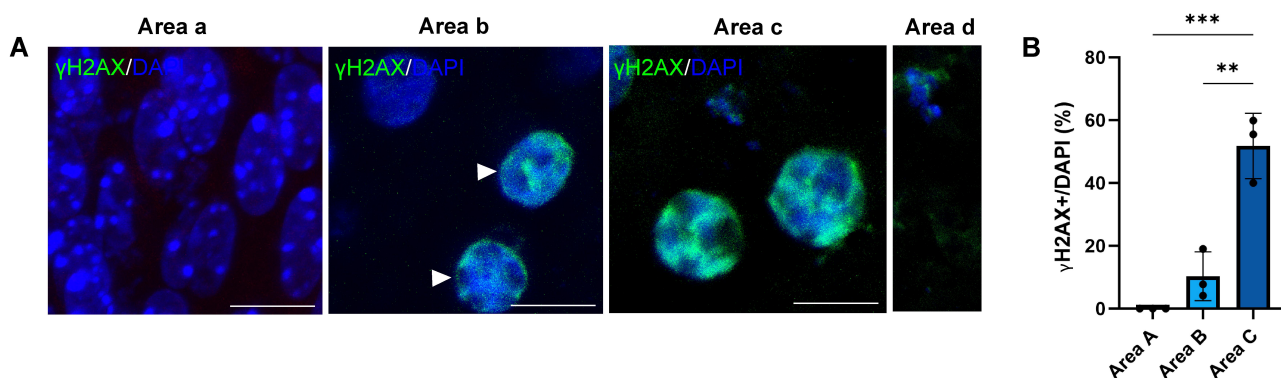
Figure 5. Analysis of DNA damage/repair prior the lens fiber cell denucleation process (P0.5). (A) The γH2AX positive nuclei are more frequently observed in areas b (white arrowheads) and c. dapi-stained nuclei (blue). (B) Quantification of γH2AX positive nuclei per total number of nuclei throughout areas a–c. Statistical significance is shown by p-values; $n = 3$ biological replicates. Scale bars = 10 μm.
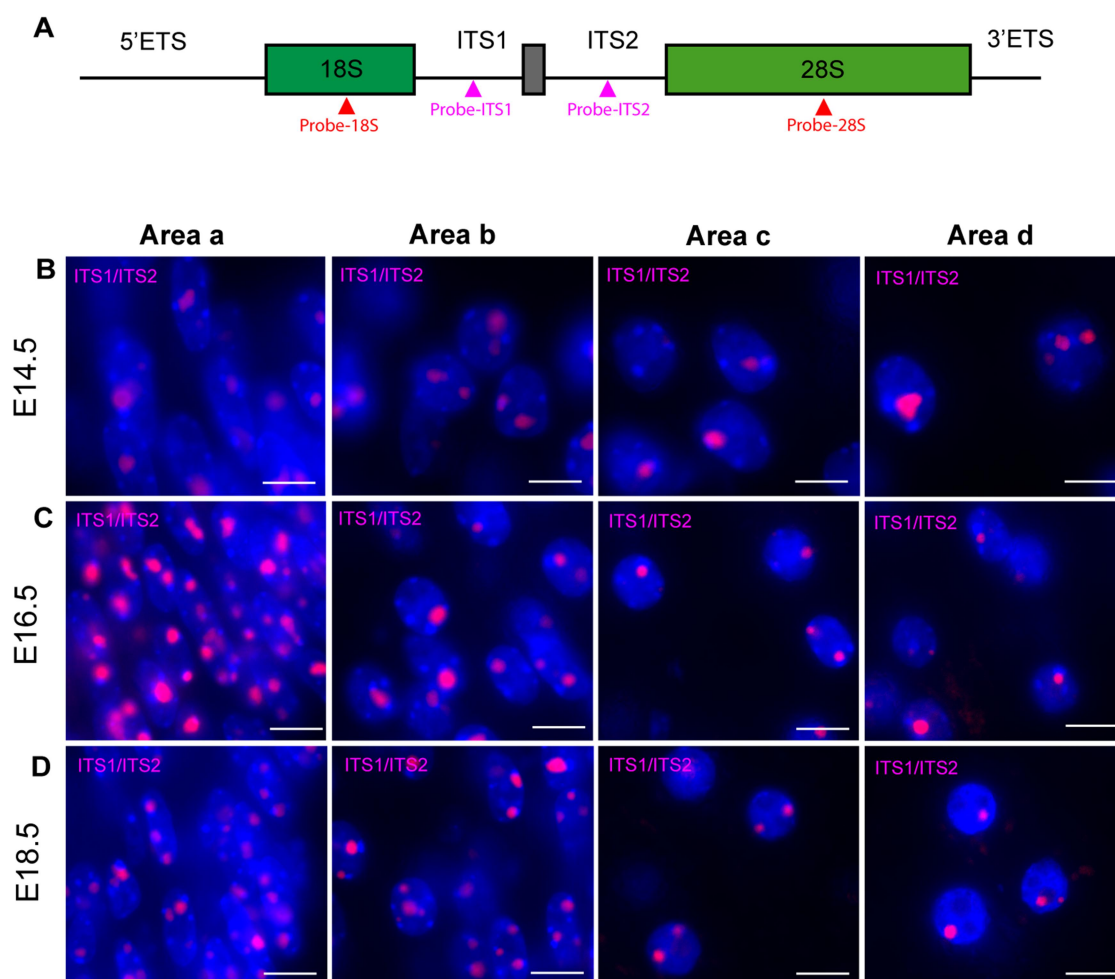

Figure 6. Visualization of nascent rRNA transcription throughout lens embryonic development (E14.5-E18.5). (A) A representative scheme of probes location in the internal-transcribed spacers 1 and 2 (ITS1/ITS2, magenta) and in the 18S and 28S (red) regions of the 47S pre-rRnas. rRNA FISH *in situ* hybridization using ITS1/ITS2 (magenta) probes was performed in embryonic lens tissue sections. (A) E14.5 fiber cells display nucleolar rRNA signal throughout areas a-d. (B) E16.5 fiber cells in area a display various nucleoli rRNA signal per nucleus. (C) E18.5 fiber cells display rRNA nucleolar signal in all areas, including area d, where condensed nuclei are observed. 5'ETS: 5'external transcribed spacer; 3'ETS: 3'external transcribed spacer. Nuclei stained with DAPI (blue). Scale bars = 5 μm.

observed in fiber cells nuclei in areas a and b, co-localizing with the nucleolus observed by DAPI counterstaining (Figure 10A,B). We have also confirmed that fiber cells in area c also show clear intranuclear staining for nucleolin and nucleophosmin (Figure 10A,B).

Discussion

The main goals of this study were to evaluate how nuclear and nucleolar morphology changes throughout the highly organized temporal-spatial patterns of lens fiber cell
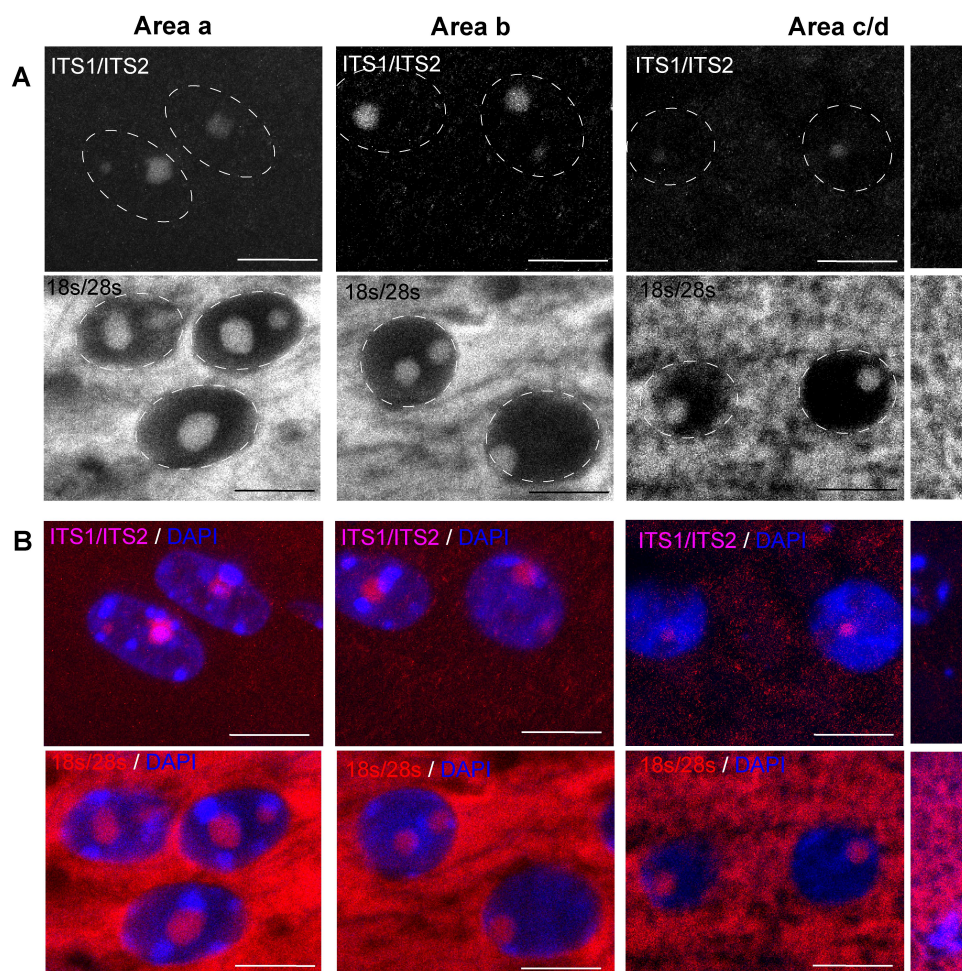
Figure 7. Visualization of nascent rRNA transcription throughout the lens fiber cell differentiation in P0.5 lenses. (A) Black and white images using ITS1/ITS2 (top) and 18S/28S (bottom) set of probes. Nucleus delineated in dotted lines. (B) Merged images of ITS1/ITS2 probes (magenta – top) and 18S/28S probes (red – bottom) and nuclei stained with DAPI (blue) in areas a, b, c and d. 5'ETS: 5'external transcribed spacer; 3'ETS: 3'external transcribed spacer. Scale bars = 10 μm.

differentiation and to determine whether rDNA transcription catalysed by RNA Polymerase I is terminated or retained throughout the entire lifespan of lens fiber cell nuclei. We thus analysed for the first time multiple nuclear and nucleolar markers and employed specific rRNA probes to visualize nascent and mature ribosomal RNAs throughout all stages of primary and secondary mouse lens fiber cell differentiation. The present data (Figures 6–8) clearly show that nascent rDNA transcription persists in lens fibre cell nuclei that are adjacent to the gradually expanding OFZ.

Mouse genetic studies of lens fibre cell denucleation revealed requirements for the lipoxygenase pathway enzyme Alox15 [57] and the lens-specific acidic DNase IIβ [58]. The latter enzymes co-localize with Lamp-1 in the lysosomes, in a specific narrow region adjacent to the OFZ [59]. Following the disassembly of the nuclear membrane, these lysosomes gain access to and degrade chromatin DNA [25]. Their nuclear entry requires cell cycle regulatory kinase Cdk1 to phosphorylate lamins A and C in addition to the nuclear mitotic apparatus protein 1 (Numa1) [40]. Parallel studies have found additional genes involved in these and other pathways, including DNA-binding transcription factors Hsf4 [60],

Gata3 [61,62] and Pax6 [63] that directly regulate expression of the *Dnase2b* gene. The denucleation process is also disrupted with inhibition of autophagy in chick lenses [64]. Retention of nuclei was also seen with lens-specific depletion of the ATP-dependent chromatin remodelling enzymes Brg1/Smarca4 [65] and Snf2h/Smarca5 [63], even though these enzymes are partially transferred into the cytoplasm in advanced lens fiber cells [23]. Interestingly, depletion of DNA repair and associated proteins Ddb1 [66], Nbs1/Nbn [67] and Ncoa6 [52] also inhibit lens fiber cell denucleation, suggesting some type of 'repurposing' of these three proteins involved in DNA repair during the denucleation process. This is further supported by the fact that active DNA repair is evident in maturing lens fiber cells from the γH2AX stainings (Figure 5).

The temporally and spatially regulated gradual changes in nuclear morphology are best viewed at P0.5 when the OFZ is already established in the central portion of the lens fiber cell compartment (Figure 1C,D). The spherical and ovoid nuclear shapes are the most common nuclear morphologies seen [68]. Nuclear rounding and transfer of proteins into the cytoplasm are characteristics shared between lens fiber cells
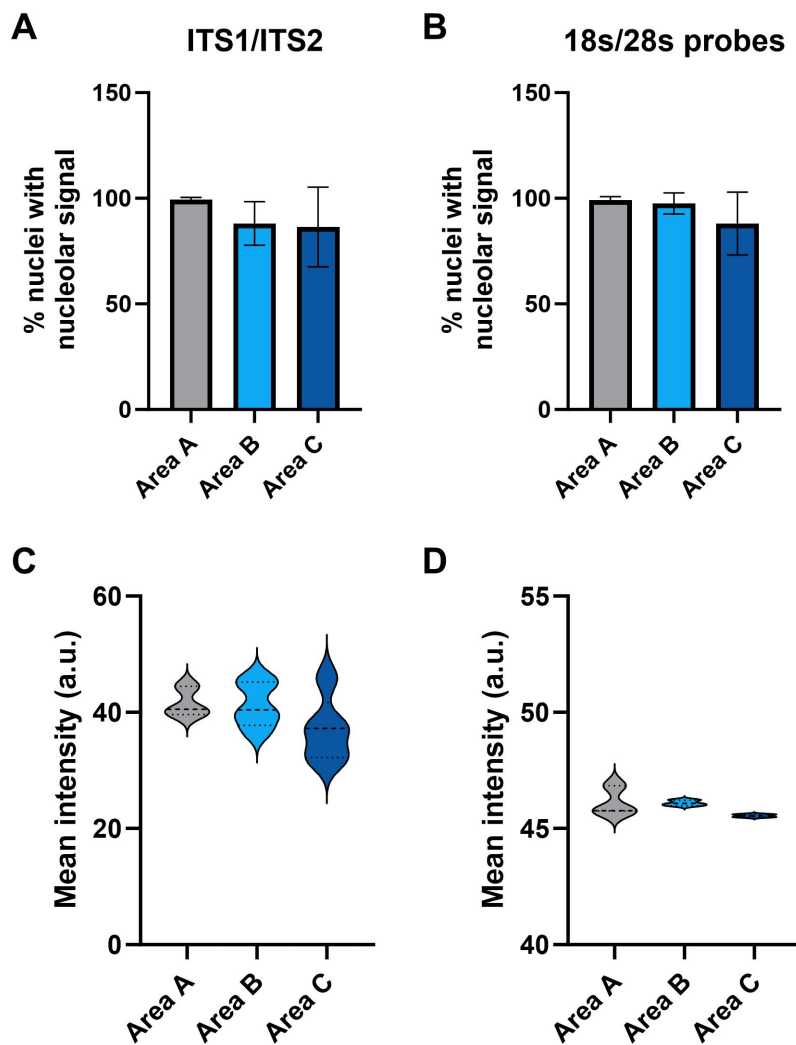
Figure 8. Quantification of nascent and mature rRNAs in lens fiber cells throughout their differentiation. (A) Quantification of nuclei (in percentage) displaying nucleolar signal for ITS1/ITS2 FISH probes in areas a, b and c. (B) Quantification of nuclei (in percentage) displaying nucleolar signal for 18S/28S FISH probes. No significant differences were observed in both groups, $n = 3$ biological replicates. (C) Under-processed rRNAs puncta's fluorescence intensity measured as signal intensity in arbitrary units (a.U.) in areas a, b and c. (D) Mature rRNAs puncta's fluorescence intensity measured as signal intensity in arbitrary units (a.U.) in areas a, b and c. Fluorescence intensity was calculated in deconvoluted images and are represented by arbitrary units (a.u.). No significant differences were observed, $n = 3$ biological replicates.

and erythrocytes [23,24]. It has been proposed that the nuclear shape and location within the cell are both affected by cellular morphology, which can further be linked to mechanical factors/constraints and driven by chromatin reorganization [68]. It is evident that locations of lens fibre cell nuclei within zones a to c are highly organized within the lens fiber cell cytoplasm (Figure 1). Importantly, lens fiber cell fusion generates a syncytium within its core and includes the OFZ [45,69]. Regarding chromatin organization, nuclear condensation is marked by a small number of large molecular condensates with transcriptionally active RNA Polymerase II that co-localize with nascent mRNA transcription of multiple crystallin genes, which are being expressed at maximum levels [23]. Most recently, our studies of the 3D-nuclear organization of lens fiber cells compared to the lens epithelium show major changes in chromatin looping within many loci that encode for

lens fibre cell structural proteins [39]. In addition, there is a remarkable redistribution of DNA-binding CTCF proteins, major organizers of chromatin looping [70]. In the lens fibre cell chromatin, ChIP-seq data show that CTCF proteins are co-localized with RNA Polymerase II [39].

The present study provides new insights into the very high transcriptional/translational outputs of lens fiber cell nuclei, especially with respect to crystallin proteins that represent as much as 90% of lens proteins (water-soluble fraction) [71]. However, multiple physiological limits still exist for these processes, including the sub-optimal delivery of nutrients to the lens via a hyaloid vascular system following its regression [35,36,72], the highly hypoxic conditions in the lens fibre cell compartment [34,73,74]) and the generation of the OFZ and abrupt nuclear degradation. Since the rRNA production highly exceeds quantities of mRNAs, it is possible that the
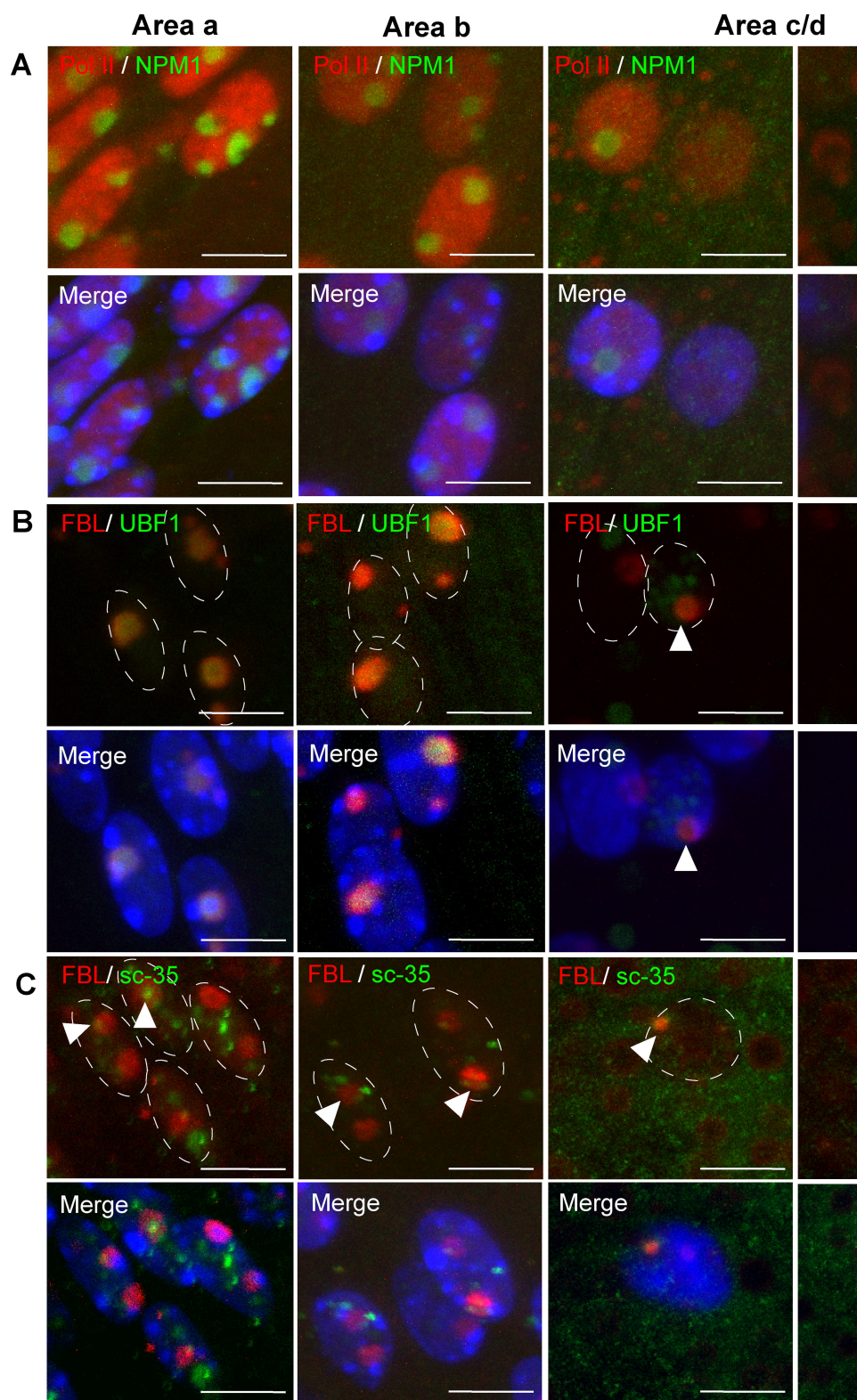
Figure 9. Nucleolar machinery is maintained prior to final nuclear disintegration (P0.5). (A) Transcriptionally active RNA polymerase II (pol II, red) signals are found in the nucleoplasm outside of the nucleoli in all the areas a, b and c. Nucleolar marker nucleophosmin (NPM1) shown in green. (B) The RNA polymerase I-specific UBF proteins (green) co-localize with nucleoli immunolabelled with fibrillarin (red) in areas a, b and c (white arrowhead). Nuclear borders are shown as dotted white lines – top. (C) The nuclear speckles detected via Sc-35 (green) signal are observed in the nucleoli immunolabelled with fibrillarin (red) within all three areas a, b and c (white arrowhead). Nuclear borders are shown in dotted white lines – top. Merge images with dapi-stained nuclei (blue). Scale bars = 10 μm.

lens fiber cells had to evolve a delicate system to find a compromise between these resource-demanding processes available for both the RNA Polymerase I and II systems [14,21,75]. One possibility is to reduce the expression of rRNAs to boost the production of crystallin mRNAs, or to reduce crystallin gene nascent transcription in favour of rRNA
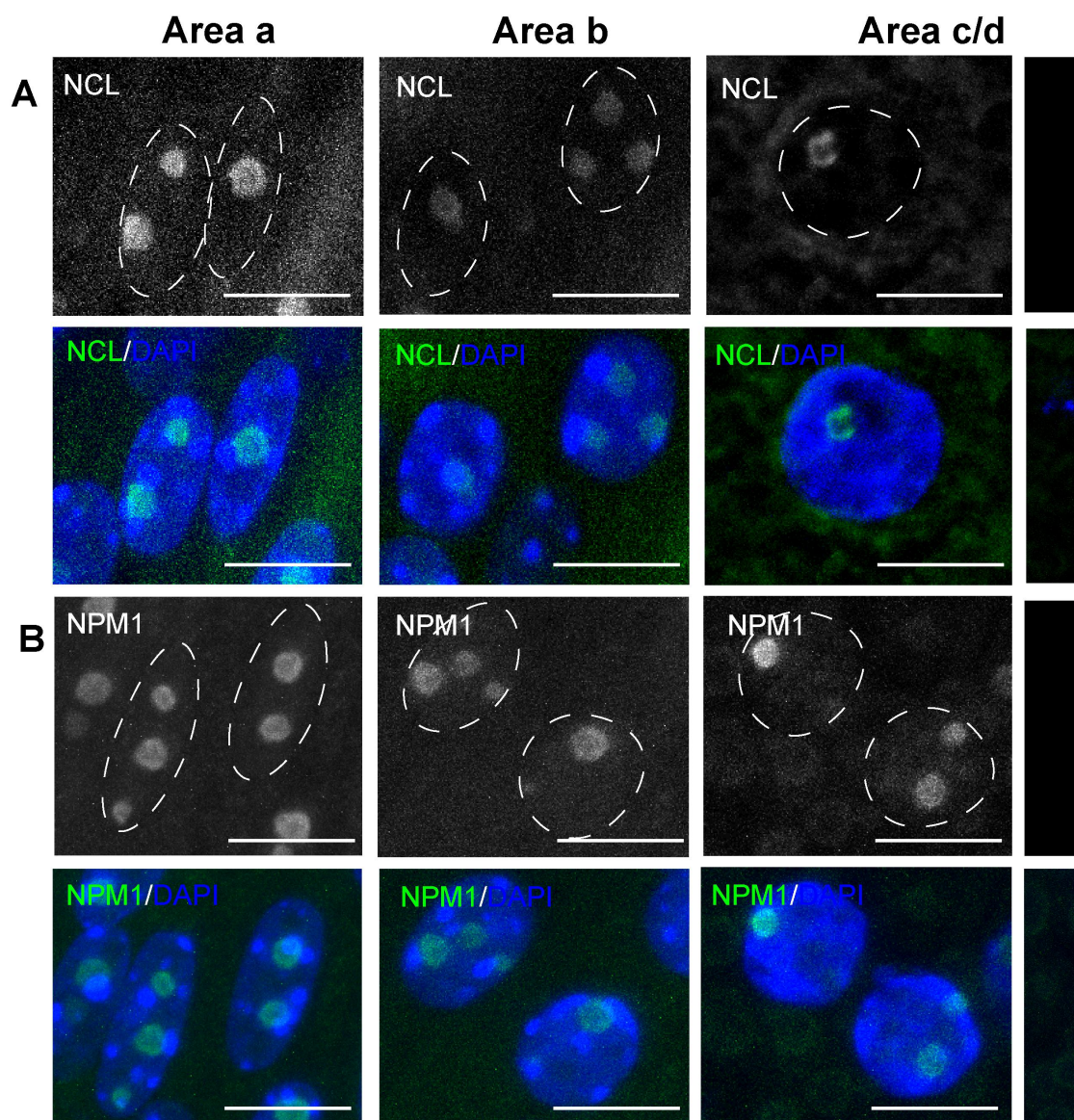
Figure 10. Essential nucleolar markers are present in fiber cells nuclei undergoing denucleation (P0.5). (A) Nucleolin (NCL) staining in newborn lens in areas a, b and c. Black and white NCL staining, nuclei depicted by dotted lines (top); NCL merged with DAPI (bottom). (B) Nucleophosmin (NPM1) staining in newborn lens in area a, b and c, nuclei depicted by white dotted lines (top); NPM1 merged with DAPI (bottom). DAPI-stained nuclei (blue). Scale bars = 10 μm.

to generate additional ribosomes. The present data clearly demonstrate that the lens fiber cell nuclei, even when approaching their degradation, are capable of high transcriptional outputs from both RNA Polymerase I and II systems. This resilience also provides indirect evidence about the functionality of molecular condensates [76–78] within the lens fiber cell nuclei again despite the fact that they are approaching their physical end. Thus, our data suggests that even though the resources within the lens fiber cells are limited at this developmental stage, the production of rRNA and mRNA remain active until the very end of the nuclear integrity as summarized in Figure 11.

In conclusion, the present studies demonstrate that denucleation during lens fiber cell differentiation is a unique model to study basic transcriptional mechanisms and chromatin organization under various highly restrictive conditions. The process of terminal denucleation will require additional mechanistic insights using a set of fluorescently marked lysosomal, nucleoplasmic and membrane proteins followed by their *in vivo* imaging. Interestingly, the translational mechanisms in both the maturing and denucleated lens fibre cells also remain to be fully established, as evidence exists about differential abundances of ribosomal proteins between the lens epithelium and lens fibers [80] and key regulatory role of subunit h of the eukaryotic translation initiation factor 3 (eIF3) in crystallin gene translation in zebrafish [81]. Thus, follow-up studies of ribosomal heterogeneity and plasticity already established in various model systems [82] are well justified in future studies of ribosomes, RNA-binding proteins interacting with crystallin mRNAs in the
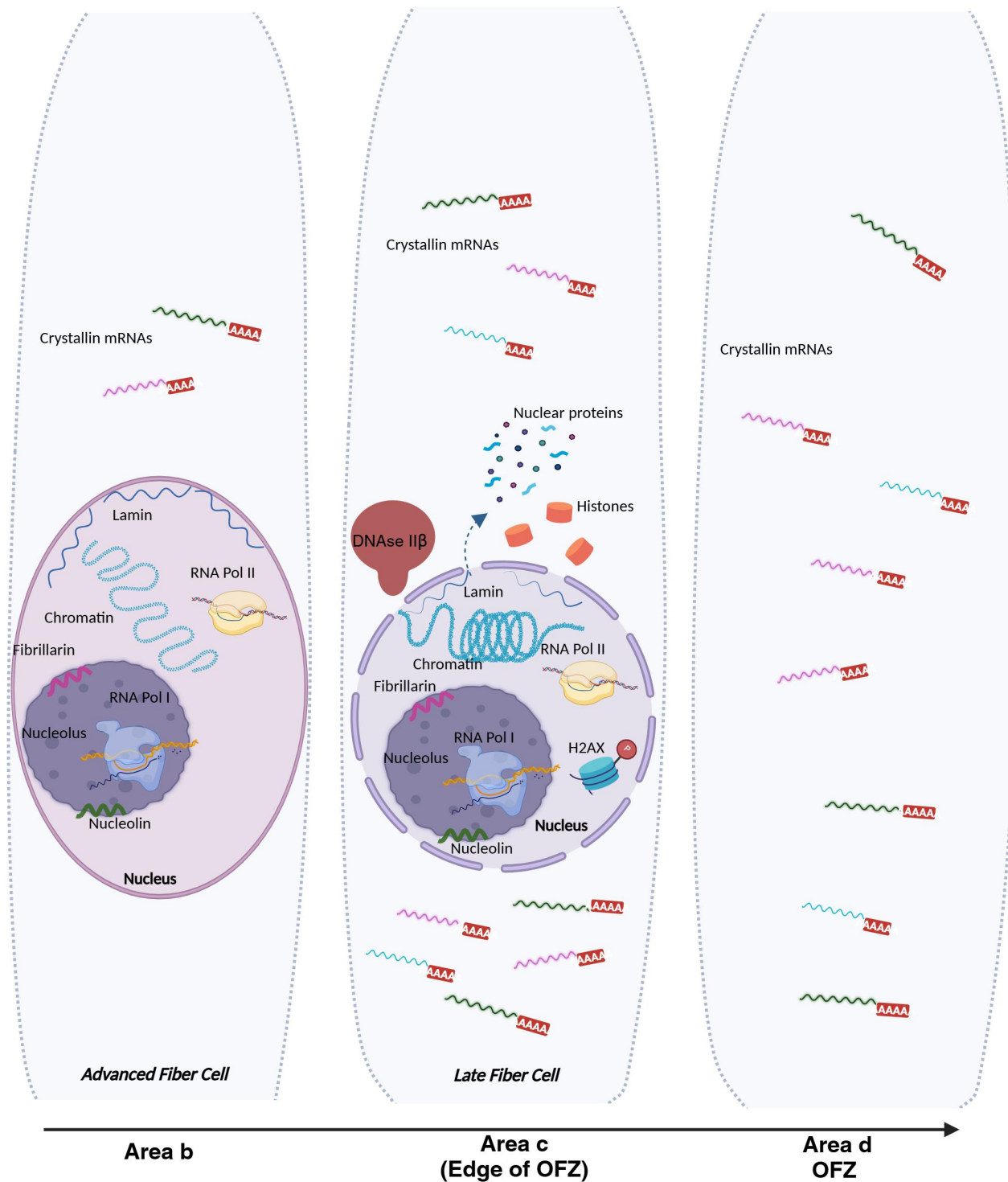
Figure 11. Summary schematic of specific features of the nuclear degradation process within differentiating lens fiber. Advanced fiber cells (P0.5) nuclei in area b are wrapped by lamin b (blue), RNA polymerases I and II generate nascent rRNAs and mRnas, and chromatin is not condensed. Nucleolar space is positive for essential nucleolar markers such as fibrillarin (pink) and nucleolin (green). Crystallin mRNAs are present in the large volume of the cytoplasm [23]. Late fiber cells at the edge of the organelle free zone (OFZ, area c) go through significant changes that include the nuclear breakdown and action of lens-specific DNase IIβ enzyme (see [27]), condensation of chromatin, and transfer of nuclear proteins and histones from the nucleus to the cytoplasm (arrow [23]. DNA damage and active repair mechanisms are linked to the increase of γH2AX phosphorylation (see Figure 5). The nucleolar space is still preserved as seen by the presence of fibrillarin and nucleolin, with RNA polymerase I is still active and crystallin mRNAs are continuously produced by RNA polymerase II [23]. Finally, the lens fiber cells within area d undergo complete abrupt nuclear disassembly and their proteins are dispersed within the large cytoplasmic volume while crystallin and other mRNAs remain intact in the cytoplasm [79].

cytoplasm [83], Cajal bodies and nuclear speckles [37,41,62] and protein translation during lens fibre cell elongation and maturation. Finally, the lens proteostasis control is directly related to lens ageing,

and lens fiber cell proteins located within the OFZ are the oldest proteins in the mammalian body [84]. This phenomenon further emphasizes the importance of regulatory mechanisms for

generating ribosomes and crystallin proteins to achieve the long-term lens transparency and function in the absence of protein turnover.

Materials and methods

Mice and tissue collection

Mouse husbandry and tissue collection were conducted in accordance with the approved protocol of the Albert Einstein College of Medicine Animal Institute Committee in addition to the ARVO statement for the use of animals in eye research. The day a vaginal plug was confirmed considered as embryonic stage E0.5. Individual eyes were harvested from embryonic days E14.5, E16.5, E18.5 and newborn (P0) CD1 mice. Females were euthanized by CO_2, mouse embryos were collected and eyes dissected. Postnatal mice were euthanized by CO_2 followed by decapitation, and eyeballs were dissected. Tissues were fixed overnight in 4% paraformaldehyde at 4°C followed by cryoprotection in 30% sucrose overnight at 4°C and embedded at optimal cutting temperature (OCT).

Immunofluorescence

Slides were kept at room temperature for 1 h followed by antigenic retrieval for 10 min at 90 degrees in citric acid solution (H3300, Vector Labs) according to manufacturer's instructions. Slides were cooled down for 10 min, and then blocked in 10% NGS (50062Z, Thermo Fisher), 1% BSA (A4737-25 G, Sigma), 0.1% Triton (9036-19-5, Sigma) in PBS for 1 h at room temperature. Slides were subsequently incubated (1:100) in blocking solution at 4°C with primary antibodies: anti-Fibrillarin (NB300-269, Novus Biologicals); anti-Lamin B (66095-1-Ig, Proteintech); anti-γH2AX (sc-377452, Santa Cruz); anti- RNA Polymerase II (ab26721, Abcam); anti-UBF1 (ab244287, Abcam); anti-SC35 (sc-53518, Santa Cruz); anti-NCL (10556-1-AP, Proteintech) and anti-NPM1 (32-5200, Thermo). After overnight incubation, slides were washed three times in PBS and incubated for 1 h at room temperature with secondary antibodies Goat anti-Rabbit IgG Alexa Fluor™ Plus 555 (A32732, Thermo) or Goat anti-Mouse IgG, Alexa Fluor™ 555 (A-21422, Thermo). Sections were washed three times in PBS, incubated 5 min at room temperature with DAPI and mounted in ProLong™ Diamond Antifade Mountant (P36961, Thermo).

Fluorescence in situ hybridization (FISH)

The procedure to generate probes for ribosomal RNA and imaging is described elsewhere [44,54]. Probes located in different regions of the 47S pre-RNA were used as described above [54]. Internal-transcribed spacers 1 and 2 (ITS1 and ITS2) enable the localization of under-processed rRNAs, whereas probes for the 18S and 28S regions localize mature pre-RNAs in the nucleus and/or cytoplasm. rRNA probes oligos were designed from the mouse pre-rRNA gene (ITS1: 3'-TAG-ACA-CGG-AAG-AGC-CGG-ACG-GGA-AAG-A- 5'-Cy3; 3'-ITS2: CCA-GCG-CAA-GAC-CCA-AAC-ACA-CAC-AGA-5'-Cy3; 18S: 3'-CCA-TTA-

TTC-CTA-GCT-GCG-GTA-TCC-AGG-CGG-5'-Cy5; 28S: 3'-GAG-GGA-ACC-AGC-TAC-TAG-ATG-GTT-CGA-TTA-5'-Cy5). Slides were immersed in Reveal Deckloaking Buffer (RV1000, Biocare Medical) at 90°C for 5 min. Subsequently, the slides were processed through several treatments to reduce tissue autofluorescence [85] and incubated in 50% formamide pre-hybridization buffer (50% formamide in 20× SSC Buffer) at 37° for 1 h. Cryosections were hybridized with 125 nM ITS1/ITS2 or 18S/28S probes overnight in a hybridization buffer (10% dextrane sulphate, 20× SSC, 50% Formamide, 10 mg/ml E. coli tRNA, 200 mm VRC, 20 mg/ml BSA) at 37°C. Post-hybridization washes with a pre-hybridization buffer were performed, followed by slide incubation with DAPI for 15 min and mounting in ProLong™ Diamond Antifade Mountant (P36961, Thermo).

Lens segmentation, imaging, quantification, statistical methods and analyses

To analyse the progression of lens fiber cell differentiation, lens tissue was symmetrically divided into four regions from the periphery to the center and were labelled as areas a, b, c and d. Area a comprises early differentiated fiber cells, area b intermediate fiber cells and area c advanced fiber cells prior to the denucleation. Area d represents disintegrating nuclei, and the organelle free zone is only observed in newborn lenses [85]. Nuclear rRNA were observed using Zeiss AxioObserver CLEM microscope. Three-dimensional image data were acquired using the Leica SP8 Confocal with the x63 oil-immersion objective plus 2.0 zoom factor. Cell quantification of the number of nuclei with nucleolar rRNA signal was conducted using ImageJ software (http://imagej.nih.gov/ij/; NIH) throughout the entire z-stack section of each image. Images were deconvoluted using Volocity software (PerkinElmer) prior to fluorescence intensity analysis, indicated by 'mean intensity (a.u.)' as we previously described [85]. At least 50 nuclei from $n = 3$ animals were analysed per segmented area. Immunofluorescence images and analysis were conducted in different tissue sections to avoid cross-reaction of antibodies. We noted a smaller number of nuclei in zone d is due to their degradation. The statistical tests used were an unpaired t test and one-way ANOVA with a multiple comparisons post-test, using GraphPad Prism 10 for Windows (www.graphpad.com; GraphPad software). Statistical significance was considered according to $p < 0.001$***; $p < 0.01$**; $p < 0.5$*.

Author contributions

CRediT: **Danielle Rayêe:** Conceptualization, Data curation, Formal analysis, Methodology, Writing – original draft, Writing – review & editing; **U. Thomas Meier:** Methodology, Writing – original draft, Writing –

ORCID

Danielle Rayêe http://orcid.org/0000-0002-8014-9854
U. Thomas Meier http://orcid.org/0000-0001-6677-2677
Carolina Eliscovich http://orcid.org/0000-0001-7653-5536
Aleš Cvekl http://orcid.org/0000-0002-3957-789X

References

[1] Roeder RG. 50+ years of eukaryotic transcription: an expanding universe of factors and mechanisms. Nat Struct Mol Biol. 2019;26 (9):783–791. doi: 10.1038/s41594-019-0287-x
[2] Feng S, Manley JL. Beyond rRNA: nucleolar transcription generates a complex network of RNAs with multiple roles in maintaining cellular homeostasis. Genes Dev. 2022;36:876–886. doi: 10. 1101/gad.349969.122
[3] Dundr M, Misteli T. Functional architecture in the cell nucleus. Biochem J. 2001;356(2):297–310. doi: 10.1042/0264-6021:3560297
[4] Lafontaine DLJ, Riback JA, Bascetin R, et al. The nucleolus as a multiphase liquid condensate. Nat Rev Mol Cell Biol. 2021;22:165–182. doi: 10.1038/s41580-020-0272-6
[5] Yoneda M, Nakagawa T, Hattori N, et al. The nucleolus from a liquid droplet perspective. J Biochem. 2021;170:153–162. doi: 10. 1093/jb/mvab090
[6] Boisvert FM, van Koningsbruggen S, Navascués J, et al. The multifunctional nucleolus. Nat Rev Mol Cell Biol. 2007;8:574–585. doi: 10.1038/nrm2184
[7] Correll CC, Bartek J, Dundr M. The nucleolus: a multiphase condensate balancing ribosome synthesis and translational capacity in health, aging and ribosomopathies. Cells. 2019;8:869. doi: 10.3390/cells8080869
[8] Correll CC, Rudloff U, Schmit JD, et al. Crossing boundaries of light microscopy resolution discerns novel assemblies in the nucleolus. Histochem Cell Biol. 2024;162(1–2):161–183. doi: 10. 1007/s00418-024-02297-7
[9] Olson MO, Dundr M, Szebeni A. The nucleolus: an old factory with unexpected capabilities. Trends Cell Biol. 2000;10:189–196. doi: 10.1016/s0962-8924(00)01738-4
[10] Hori Y, Engel C, Kobayashi T. Regulation of ribosomal RNA gene copy number, transcription and nucleolus organization in eukaryotes. Nat Rev Mol Cell Biol. 2023;24(6):414–429. doi: 10. 1038/s41580-022-00573-9
[11] McStay B. Nucleolar organizer regions: genomic 'dark matter' requiring illumination. Genes Dev. 2016;30(14):1598–1610. doi: 10.1101/gad.283838.116
[12] Granneman S, Baserga SJ. Crosstalk in gene expression: coupling and co-regulation of rDNA transcription, pre-ribosome assembly and pre-rRNA processing. Curr Opin Cell Biol. 2005;17:281–286. doi: 10.1016/j.ceb.2005.04.001
[13] Zentner GE, Balow SA, Scacheri PC. Genomic characterization of the mouse ribosomal DNA locus. G3 (Bethesda. G3 Genes|genomes|genet. 2014;4(2):243–254. doi: 10.1534/g3.113.009290
[14] Cerqueira AV, Lemos B. Ribosomal DNA and the nucleolus as keystones of nuclear architecture, organization, and function. Trends Genet. 2019;35(10):710–723. doi: 10.1016/j.tig.2019.07.011
[15] Cech TR, Steitz JA. The noncoding RNA revolution-trashing old rules to forge new ones. Cell. 2014;157:77–94. doi: 10.1016/j.cell.2014.03.008
[16] Willis IM, Moir RD. Signaling to and from the RNA polymerase III transcription and processing machinery. Ann Rev Biochem. 2018;87:75–100. doi: 10.1146/annurev-biochem-062917-012624
[17] White RJ. Transcription by RNA polymerase III: more complex than we thought. Nat Rev Genet. 2011;12:459–463. doi: 10.1038/nrg3001
[18] Wu J, Xiao J, Zhang Z, et al. Ribogenomics: the science and knowledge of RNA. Genomics Proteomics Bioinformatics. 2014;12(2):57–63. doi: 10.1016/j.gpb.2014.04.002
[19] Vermunt MW, Zhang D, Blobel GA. The interdependence of gene-regulatory elements and the 3D genome. J Cell Biol. 2018;218:12–26. doi: 10.1083/jcb.201809040
[20] Misteli T. The self-organizing genome: principles of genome architecture and function. Cell. 2020;183:28–45. doi: 10.1016/j. cell.2020.09.014
[21] Grummt I, Ladurner AG. A metabolic throttle regulates the epigenetic state of rDNA. Cell. 2008;133(4):577–580. doi: 10.1016/j. cell.2008.04.026
[22] Ni C, Buszczak M. The homeostatic regulation of ribosome biogenesis. Semin Cell Dev Biol. 2023;136:13–26. doi: 10.1016/j. semcdb.2022.03.043
[23] Limi S, Senecal A, Coleman R, et al. Transcriptional burst fraction and size dynamics during lens fiber cell differentiation and detailed insights into the denucleation process. J Biol Chem. 2018;293(34):13176–13190. doi: 10.1074/jbc.RA118.001927
[24] Zhao B, Mei Y, Schipma MJ, et al. Nuclear condensation during Mouse Erythropoiesis requires Caspase-3-mediated nuclear opening. Dev Cell. 2016;36(5):498–510. doi: 10.1016/j.devcel.2016.02.001
[25] Bassnett S. On the mechanism of organelle degradation in the vertebrate lens. Exp Eye Res. 2009;88(2):133–139. doi: 10.1016/j. exer.2008.08.017
[26] Rowan S, Chang ML, Reznikov N, et al. Disassembly of the lens fiber cell nucleus to create a clear lens: the p27 descent. Exp Eye Res. 2017;156:72–78. doi: 10.1016/j.exer.2016.02.011
[27] Brennan L, Disatham J, Kantorow M. Mechanisms of organelle elimination for lens development and differentiation. Exp Eye Res. 2021;209:108682. doi: 10.1016/j.exer.2021.108682
[28] Rogerson C, Bergamaschi D, Rfl O. Uncovering mechanisms of nuclear degradation in keratinocytes: a paradigm for nuclear degradation in other tissues. Nucleus. 2018;9:56–64. doi: 10. 1080/19491034.2017.1412027
[29] Cvekl A, Eliscovich C. Crystallin gene expression: insights from studies of transcriptional bursting. Exp Eye Res. 2021;207:108564. doi: 10.1016/j.exer.2021.108564
[30] Sun J, Rockowitz S, Chauss D, et al. Chromatin features, RNA polymerase II and the comparative expression of lens genes encoding crystallins, transcription factors, and autophagy mediators. Mol Vis. 2015;21:955–973. PMID: 26330747.
[31] Grummt I. Life on a planet of its own: regulation of RNA polymerase I transcription in the nucleolus. Genes Dev. 2003;17:1691–1702. doi: 10.1101/gad.1098503R
[32] Shore D, Albert B. Ribosome biogenesis and the cellular energy economy. Curr Biol. 2022;32:R611–R617. doi: 10.1016/j.cub.2022.04.083
[33] Brennan LA, McGreal-Estrada R, Logan CM, et al. BNIP3L/NIX is required for elimination of mitochondria, endoplasmic reticulum and Golgi apparatus during eye lens organelle-free zone formation. Exp Eye Res. 2018;174:173–184. doi: 10.1016/j.exer.2018.06.003
[34] Beebe DC. Maintaining transparency: a review of the developmental physiology and pathophysiology of two avascular tissues. Semin Cell Dev Biol. 2008;19:125–133. doi: 10.1016/j.semcdb.2007.08.014

[35] Chen Y, Doughman YQ, Gu S, et al. Cited2 is required for the proper formation of the hyaloid vasculature and for lens morphogenesis. Development. 2008;135:2939–2948. doi: 10.1242/dev.021097

[36] McKeller RN, Fowler JL, Cunningham JJ, et al. The arf tumor suppressor gene promotes hyaloid vascular regression during mouse eye development. Proc Natl Acad Sci USA. 2002;99:3848–3853. doi: 10.1073/pnas.05248419

[37] Dahm R, Gribbon C, Quinlan RA, et al. Changes in the nucleolar and coiled body compartments precede lamina and chromatin reorganization during fibre cell denucleation in the bovine lens. Eur J Cell Biol. 1998;75(3):237–246. doi: 10.1016/S0171-9335(98)80118-0

[38] Bassnett S, Mataic D. Chromatin degradation in differentiating fiber cells of the eye lens. J Cell Bio. 1997;137(1):37–49. doi: 10.1083/jcb.137.1.37

[39] Camerino M, Chang W, Cvekl A. Analysis of long-range chromatin contacts, compartments and looping between mouse embryonic stem cells, lens epithelium and lens fibers. Epigenetics Chromatin. 2024;17:10. doi: 10.1186/s13072-024-00533-x

[40] Chaffee BR, Shang F, Chang ML, et al. Nuclear removal during terminal lens fiber cell differentiation requires CDK1 activity: appropriating mitosis-related nuclear disassembly. Development. 2014;141(17):3388–3398. doi: 10.1242/dev.106005

[41] Gribbon C, Dahm R, Prescott AR, et al. Association of the nuclear matrix component NuMA with the Cajal body and nuclear speckle compartments during transitions in transcriptional activity in lens cell differentiation. Eur J Cell Biol. 2002;81(10):557–566. doi: 10.1078/0171-9335-00275

[42] Kuwabara T, Imaizumi M. Denucleation process of the lens. Invest Ophthalmol Vis Sci. 1974;13:973–981.

[43] Faulkner-Jones B, Zandy AJ, Bassnett S. RNA stability in terminally differentiating fibre cells of the ocular lens. Exp Eye Res. 2003;77:463–476. doi: 10.1016/S0014-4835(03)00172-6

[44] Qian J, Lavker RM, Tseng H. Mapping ribosomal RNA transcription activity in the mouse eye. Dev Dyn. 2006;235(7):1984–1993. doi: 10.1002/dvdy.20827

[45] Shi Y, Barton K, De Maria A, et al. The stratified syncytium of the vertebrate lens. J Cell Sci. 2009;122(10):1607–1615. doi: 10.1242/jcs.045203

[46] Cheng C, Nowak RB, Fowler VM. The lens actin filament cytoskeleton: diverse structures for complex functions. Exp Eye Res. 2017;156:58–71. doi: 10.1016/j.exer.2016.03.005

[47] Rao PV, Maddala R. The role of the lens actin cytoskeleton in fiber cell elongation and differentiation. Semin Cell Dev Biol. 2006;17:698–711. doi: 10.1016/j.semcdb.2006.10.011

[48] Cvekl A, Zhang X. Signaling and gene regulatory networks in mammalian lens development. Trends Genet. 2017;33:677–702. doi: 10.1016/j.tig.2017.08.001

[49] Scott DD, Oeffinger M. Nucleolin and nucleophosmin: nucleolar proteins with multiple functions in DNA repair. Biochem Cell Biol. 2016;94:419–432. doi: 10.1139/bcb-2016-0068

[50] Ma N, Matsunaga S, Takata H, et al. Nucleolin functions in nucleolus formation and chromosome congression. J Cell Sci. 2007;120:2091–2105. doi: 10.1242/jcs.008771

[51] Gheyas R, Menko AS. The involvement of caspases in the process of nuclear removal during lens fiber cell differentiation. Cell Death Discov. 2023;9:386. doi: 10.1038/s41420-023-01680-y

[52] Wang WL, Li Q, Xu J, et al. Lens fiber cell differentiation and denucleation are disrupted through expression of the N-terminal nuclear receptor box of NCOA6 and result in p53-dependent and p53-independent apoptosis. Mol Biol Cell. 2010;21:2453–2468. doi: 10.1091/mbc.e09-12-1031

[53] Economopoulou M, Langer H, Celeste A, et al. Histone H2AX is integral to hypoxia-driven neovascularization. Nat Med. 2009;15:553–558. doi: 10.1038/nm.1947

[54] Chebrout M, Koné MC, Jan HU, et al. Transcription of rRNA in early mouse embryos promotes chromatin reorganization and expression of major satellite repeats. J Cell Sci. 2022;135(6):jcs258798. doi: 10.1242/jcs.258798

[55] Theophanous A, Christodoulou A, Mattheou C, et al. Transcription factor UBF depletion in mouse cells results in downregulation of both downstream and upstream elements of the rRNA transcription network. J Biol Chem. 2023;299(10):105203. doi: 10.1016/j.jbc.2023.105203

[56] Spector DL, Lamond AI. Nuclear speckles. Cold Spring Harb Perspect Biol. 2011;3(2):a000646. doi: 10.1101/cshperspect.a000646

[57] Van Leyen K, Duvoisin RM, Engelhardt H, et al. A function for lipoxygenase in programmed organelle degradation. Nature. 1998;395:392–395. doi: 10.1038/26500

[58] Nishimoto S, Kawane K, Watanabe-Fukunaga R, et al. Nuclear cataract caused by a lack of DNA degradation in the mouse eye lens. Nature. 2003;424(6952):1071–1074. doi: 10.1038/nature01895

[59] Nakahara M, Nagasaka A, Koike M, et al. Degradation of nuclear DNA by DNase ii-like acid DNase in cortical fiber cells of mouse eye lens. FEBS J. 2007;274:3055–3064. doi: 10.1111/j.1742-4658.2007.05836.x

[60] Fujimoto M, Izu H, Seki K, et al. HSF4 is required for normal cell growth and differentiation during mouse lens development. Embo J. 2004;23(21):4297–4306. doi: 10.1038/sj.emboj.7600435

[61] Maeda A, Moriguchi T, Hamada M, et al. Transcription factor GATA-3 is essential for lens development. Dev Dyn. 2009;238:2280–2291. doi: 10.1002/dvdy.22035

[62] Martynova E, Zhao Y, Xie Q, et al. Transcriptomic analysis and novel insights into lens fibre cell differentiation regulated by Gata3. Open Biol. 2019;9:190220. doi: 10.1098/rsob.190220

[63] He S, Limi S, McGreal RS, et al. Chromatin remodeling enzyme Snf2h regulates embryonic lens differentiation and denucleation. Development. 2016;143(11):1937–1947. doi: 10.1242/dev.135285

[64] Basu S, Rajakaruna S, Reyes B, et al. Suppression of MAPK/JNK-MTORC1 signaling leads to premature loss of organelles and nuclei by autophagy during terminal differentiation of lens fiber cells. Autophagy. 2014;10:1193–1211. doi: 10.4161/auto.28768

[65] He S, Pirity MK, Wang WL, et al. Chromatin remodeling enzyme Brg1 is required for mouse lens fiber cell terminal differentiation and its denucleation. Epigenetics Chromatin. 2010;3(1):21. doi: 10.1186/1756-8935-3-21

[66] Cang Y, Zhang J, Nicholas SA, et al. Deletion of DDB1 in mouse brain and lens leads to p53-dependent elimination of proliferating cells. Cell. 2006;127(5):929–940. doi: 10.1016/j.cell.2006.09.045

[67] Yang YG, Frappart PO, Frappart L, et al. A novel function of DNA repair molecule Nbs1 in terminal differentiation of the lens fibre cells and cataractogenesis. DNA Repair (Amst). 2006;5(8):885–893. doi: 10.1016/j.dnarep.2006.05.004

[68] Webster M, Witkin KL, Cohen-Fix O. Sizing up the nucleus: nuclear shape, size and nuclear-envelope assembly. J Cell Sci. 2009;122(10):1477–1486. doi: 10.1242/jcs.037333

[69] Mathias RT, Rae JL, Eisenberg RS. The lens as a nonuniform spherical syncytium. Biophys J. 1981;34:61–83. doi: 10.1016/S0006-3495(81)84837-0

[70] Ghirlando R, Felsenfeld G. CTCF: making the right connections. Genes Dev. 2016;30(8):881–891. doi: 10.1101/gad.277863.116

[71] Bassnett S, Shi Y, Vrensen GF. Biological glass: structural determinants of eye lens transparency. Philos Trans R Soc Lond B Biol Sci. 2011;366(1568):1250–1264. doi: 10.1098/rstb.2010.0302

[72] Lang RA. Apoptosis in mammalian eye development: lens morphogenesis, vascular regression and immune privilege. Cell Death Differ. 1997;4:12–20. doi: 10.1038/sj.cdd.4400211

[73] Brennan L, Disatham J, Kantorow M. Hypoxia regulates the degradation of non-nuclear organelles during lens differentiation through activation of HIF1a. Exp Eye Res. 2020;198:108129. doi: 10.1016/j.exer.2020.108129

[74] Shui YB, Beebe DC. Age-dependent control of lens growth by hypoxia. Invest Ophthalmol Vis Sci. 2008;49:10023–11029. doi: 10.1167/iovs.07-1164

[75] Daiß JL, Griesenbeck J, Tschochner H, et al. Synthesis of the ribosomal RNA precursor in human cells: mechanisms, factors and regulation. Biol Chem. 2023;404:1003–1023. doi: 10.1515/hsz-2023-0214

[76] Banani SF, Lee HO, Hyman AA, et al. Biomolecular condensates: organizers of cellular biochemistry. 2017. Nat Rev Mol Cell Biol. 2017;18(5):285–298. doi: 10.1038/nrm.2017.7

[77] Brangwynne CP, Mitchison TJ, Hyman AA. Active liquid-like behavior of nucleoli determines their size and shape in *Xenopus laevis*

oocytes. Proc Natl Acad Sci U S A. 2011;108(11):4334–4339. doi: 10.1073/pnas.1017150108

[78] Sharp PA, Chakraborty AK, Henninger JE, et al. RNA in formation and regulation of transcriptional condensates. RNA. 2021;28:52–57. doi: 10.1261/rna.078997.121

[79] Gangalum RK, Kim D, Kashyap RK, et al. Spatial analysis of single fiber cells of the developing ocular lens reveals regulated heterogeneity of gene expression. iScience. 2018;21:66–79. doi: 10.1016/j.isci.2018.11.024

[80] Zhao Y, Wilmarth PA, Cheng C, et al. Proteome-transcriptome analysis and proteome remodeling in mouse lens epithelium and fibers. Exp Eye Res. 2019;179:32–46. doi: 10.1016/j.exer.2018.10.011

[81] Choudhuri A, Maitra U, Evans T. Translation initiation factor eIf3h targets specific transcripts to polysomes during embryogenesis. Proc Natl Acad Sci USA. 2013;110(24):9818–9823. doi: 10.1073/pnas.1302934110

[82] Trahan C, Oeffinger M. The importance of being RNA-est: considering RNA-mediated ribosome plasticity. RNA Biol. 2023;20(1):177–185. doi: 10.1080/15476286.2023.2204581

[83] Rayêe D, Hwang DW, Chang WK, et al. Identification and classification of abundant RNA-binding proteins in the mouse lens and interactions of Carhsp1, Igf2bp1/ZBP1, and Ybx1 with crystallin and β-actin mRNAs. bioRxiv 2025: 2025–01. 2025. doi: 10.1101/2025.01.10.632466

[84] Cvekl A, Vijg J. Aging of the eye: lessons from cataracts and age-related macular degeneration. Ageing Res Rev. 2024;6:102407. doi: 10.1016/j.arr.2024.102407

[85] Limi S, Zhao Y, Guo P, et al. Bidirectional analysis of Cryba4-Crybb1 nascent transcription and nuclear accumulation of Crybb3 mRNAs in lens fibers. Invest Ophthalmol Vis Sci. 2019;60(1):234–244. doi: 10.1167/iovs.18-25921